P
06304B

NASA TECHNICAL NOTE

NASA TN D-3182

NASA TN D-3182

AMPTIAC

DISTRIBUTION STATEMENT A
Approved for Public Release
Distribution Unlimited

STATIC AERODYNAMIC CHARACTERISTICS OF A ROCKET VEHICLE WITH THICK WEDGE FINS AND SWEPTBACK LEADING AND TRAILING EDGES

by Joseph A. Yuska

Lewis Research Center

Cleveland, Ohio

20060516205

NATIONAL AERONAUTICS AND SPACE ADMINISTRATION • WASHINGTON, D. C. • JANUARY 1966

NASA TN D-3182

STATIC AERODYNAMIC CHARACTERISTICS OF A ROCKET VEHICLE WITH THICK WEDGE FINS AND SWEPTBACK LEADING AND TRAILING EDGES

By Joseph A. Yuska

Lewis Research Center
Cleveland, Ohio

NATIONAL AERONAUTICS AND SPACE ADMINISTRATION

For sale by the Clearinghouse for Federal Scientific and Technical Information
Springfield, Virginia 22151 – Price $1.00

STATIC AERODYNAMIC CHARACTERISTICS OF A ROCKET VEHICLE WITH THICK WEDGE FINS WITH SWEPTBACK LEADING AND TRAILING EDGES

by Joseph A. Yuska

Lewis Research Center

SUMMARY

The longitudinal static stability characteristics of three one-fifth scale models of the second stage of a sounding rocket were calculated and compared with the measured values at Mach numbers of 1.79 to 3.47. All three models had fins of trapezoidal planform with sweptback leading and trailing edges, small aspect ratio, and thick wedge sections, but differed in fin area and overall model length. Calculations of center of pressure and normal-force coefficient slope at zero normal force were in good agreement with experimental data.

INTRODUCTION

During the aerodynamic design of a two-stage sounding rocket having a long payload compartment, it was found necessary to propose the use of fins having a trapezoidal planform with sweptback leading and trailing edges, small aspect ratio, and a thick wedge section to obtain adequate static stability of the second stage at high supersonic speeds.

A general method (ref. 1) for calculating the normal-force slope coefficient and the center of pressure for a wing-body combination is well established, but the authors state that the method is restricted to configurations having trailing edges that are not swept back and also that some successful preliminary correlations between data and estimates by their method have been made for configurations having trailing edges that are not swept back. A literature search revealed little additional specific information or data at supersonic Mach numbers on wing-body combinations having fins similar to the proposed sounding rocket configuration. Therefore, it was desired to determine if the supersonic longitudinal static stability characteristics of the proposed sounding rocket could be calculated successfully by using the method of reference 1 and accounting for the increased lift of the wedge section by including the wedge effectiveness factor as described in reference 2.

Three one-fifth scale models of the rocket were tested between Mach num-

bers of 1.79 and 3.47 in the Lewis 10- by 10-foot and 8- by 6-foot supersonic wind tunnels. The test data were compared to results of static stability calculations by the method mentioned previously.

SYMBOLS

C_A	axial-force coefficient, axial force/qS
C_M	pitching-moment coefficient, pitching moment/qSd, measured about base of model
C_{M_α}	pitching-moment coefficient slope at zero normal force, $\partial C_M/\partial\alpha$ per radian
C_N	normal-force coefficient, normal force/qS
C_{N_α}	normal-force coefficient slope at zero normal force, $\partial C_N/\partial\alpha$ per radian
d	reference length, body diameter, 0.5 ft
l_m	distance from station 0 to model base, ft
M_O	free-stream Mach number
q	dynamic pressure, lb/sq ft
S	reference area, cross-sectional body area, 0.1964 sq ft
$\overline{X}_{cp}/d$	center of pressure at zero normal force, measured from station 0, calibers
α	angle of attack, deg

APPARATUS AND PROCEDURE

Three models were used during this investigation, all having an approximately three-quarter power nose followed by a 6-inch-diameter cylindrical section having four wedge fins which were canted at 0.8°. The model nose coordinates are given in figure 1. Model A, shown in figure 1, was 65.9 inches long and had a fin planform area of 77.66 square inches. Model B was derived from model A by shortening the model to 61.7 inches by removing the cylindrical section A shown in figure 1. Model C was obtained from model A by reducing the fin planform area from 77.66 to 70.34 square inches by removing section B (fig. 1).

Axial and normal forces on the model were measured with a calibrated three-component bearing-type strain gage balance mounted inside the model at approximately the center of pressure as shown in figure 1. The balance was then sting mounted to the tunnel central support system. A photograph of model B in the 10- by 10-foot supersonic wind tunnel is shown in figure 2. The model angle of attack was measured directly by a strain-gage pendulum-type angle-of-attack transducer mounted in the nose of the model. The base and cavity pressure taps shown in figure 1 were used to obtain actual base drag, which was subtracted from the balance drag.

The models were tested through Mach number ranges of 1.79 to 2.08 in the 8- by 6-foot supersonic wind tunnel and 2.0 to 3.47 in the 10- by 10-foot supersonic wind tunnel with angles of attack varying from -3.0° to 10.0°. Model test parameters are shown in table I and tunnel conditions in table II.

RESULTS AND DISCUSSION

Experimental Results

Typical curves of normal-force and pitching-moment coefficients plotted against angle of attack for all tests are presented in figure 3. It can be seen from figure 3 that C_N and C_M are not zero at zero measured angle of attack. In the case of the data obtained in the 10- by 10-foot supersonic wind tunnel (figs. 3(a), (c), (d), and (e)) the errors in the data could be attributed to inaccuracies in the measured angle of attack combined with flow angularity. In the case of the data obtained in the 8- by 6-foot supersonic wind tunnel the consistency of error suggests either a flow angularity effect or a direct effect on the balance normal-force link produced by errors in the fin cant angle.

The C_{N_α} and C_{M_α} data used to prepare C_{N_α} and $\bar{X}_{cp}/d$ curves were obtained by fitting a straight line by the method of least squares through the data of figure 3 between angles of attack of -3° and 4°.

By definition, the center of pressure measured in calibers from station 0 is

$$\frac{\bar{X}_{cp}}{d} = \frac{l_m}{d} - \frac{C_M}{C_N} \tag{1}$$

This equation, however, becomes indeterminate at zero angle of attack because in theory C_M and C_N are zero. Also, the percentage errors in measured C_N and C_M increase near zero angle of attack. Therefore, the center of pressure at zero angle of attack is more accurately obtained by differentiating equation (1) with respect to α and using the slopes of the C_N and C_M curves to obtain

$$\frac{\bar{X}_{cp}}{d} = \frac{l_m}{d} - \frac{C_{M_\alpha}}{C_{N_\alpha}} \tag{2}$$

The experimental center of pressure calculated by equation (2) and the normal-force coefficient slope are shown in figure 4.

The axial-force coefficients at zero measured angle of attack are plotted against Mach number in figure 5. The axial-force coefficients have been adjusted to a condition of free-stream static pressure at the base of the model and therefore represent power-on axial-force coefficients, assuming there is a jet issuing from the entire base of the model. As expected, the axial-force coefficients of models A and B were about the same since the only difference in the models was the cylindrical length and model B would have only slightly less skin-friction drag. The axial-force coefficients of model C were significantly less than the axial-force coefficients of models A and B because of the smaller fin area.

Comparison of Theoretical and Experimental

Static Stability Characteristics

The plots of normal-force coefficient and center of pressure against Mach number for the wing-body combination were calculated by the method of reference 1, which is the summation of forces and moments of the various geometric shapes with interference which make up the model configuration. The normal-force coefficient slope for the fin alone was obtained by using the experimental and theoretical data of reference 3 and applying the wedge effectiveness factor of reference 2 to the fin normal-force coefficient slope to account for the increased lift of the wedge section at supersonic speeds. This method of calculation has been applied successfully at a Mach number of 4.65 to a wing-body combination having wedge delta fins (ref. 4).

As can be seen from figure 4, good agreement between calculated values and experimental data was obtained for all models, 9 and -7 percent for the normal-force coefficient slope and ±1.5 percent of the body length for the center-of-pressure location at zero normal force. The correlation of theoretical calculations and experimental data for C_{N_α} and $\bar{X}_{cp}/d$ as stated in reference 1 is ±10 percent for the normal-force coefficient and ±2 percent of the body length for the center-of-pressure location at zero normal force. Thus, the accuracy of the calculations of this report, which include the wedge effectiveness factor of reference 2, seems to be as good as that of the calculations of reference 1; however, as previously discussed, the method is restricted to configurations having trailing edges that are not swept back. Figure 6 shows the effect of excluding the wedge effectiveness factor from the calculations.

CONCLUDING REMARKS

Three one-fifth scale models of the second stage of a sounding rocket were tested between Mach numbers of 1.79 and 3.47 and angles of attack of -3° and 10° in the Lewis 10- by 10-foot and 8- by 6-foot supersonic wind tunnels. All models had an approximately three-quarter-power nose followed by a cylindrical section having four fins of trapezoidal planform with sweptback leading and trailing edges, small aspect ratio, and a thick wedge section. The models differed in fin area and overall model length.

The normal-force coefficient slope and the center of pressure were measured for each model. It was found that the estimates of these parameters, based on the calculation method of reference 1 and including the wedge effectiveness factor of reference 2, were in good agreement with the data, although the method of reference 1 is reported to be restricted to configurations having trailing edges not swept back.

Lewis Research Center,
National Aeronautics and Space Administration,
Cleveland, Ohio, October 4, 1965.

REFERENCES

1. Pitts, William C.; Nielsen, Jack N.; and Kaattari, George E.: Lift and Center of Pressure of Wing-Body-Tail Combinations at Subsonic, Transonic, and Supersonic Speeds. NACA TR 1307, 1957.

2. McLellan, Charles H.: A Method for Increasing the Effectiveness of Stabilizing Surfaces at High Supersonic Mach Numbers. NACA RM L54F21, 1954.

3. Malthan, L. V. ed.: USAF Stability and Control Handbook. Pt I. McGregor and Werner, Inc., 1961.

4. Keynton, Robert J.: Static Longitudinal Stability of a Rocket Vehicle Having a Rear-Facing Step Ahead of the Stabilizing Fins. NASA TN D-993, 1961.

TABLE I. - MODEL TEST PARAMETERS

Test	Model	Model length, in.	Fin planform area, sq in.	Model roll position, deg	Wind tunnel
1	A	65.9	77.66	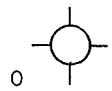 0	10- by 10-ft
1A	A	65.9	77.66	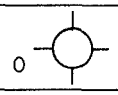 0	8- by 6-ft
2	A	65.9	77.66	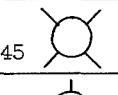 45	10- by 10-ft
3	B	61.7	77.66	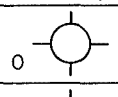 0	10- by 10-ft
4	C	65.9	70.34	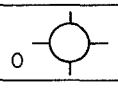 0	10- by 10-ft

TABLE II. - TEST CONDITIONS

Mach number	Total pressure, lb/sq ft abs	Dynamic pressure, lb/sq ft	Reynolds number per foot
10- By 10-foot supersonic wind tunnel			
2.00	1430	511	2.49×10^6
2.09	1492	507	2.48
2.38	1725	482	2.47
2.78	2545	522	2.34
3.17	3570	529	2.41
3.47	4695	544	2.47
8- By 6-foot supersonic wind tunnel			
1.79	3140	1240	5.03×10^6
1.88	3330	1268	5.0
1.98	3548	1284	4.9
2.08	3739	1353	5.03

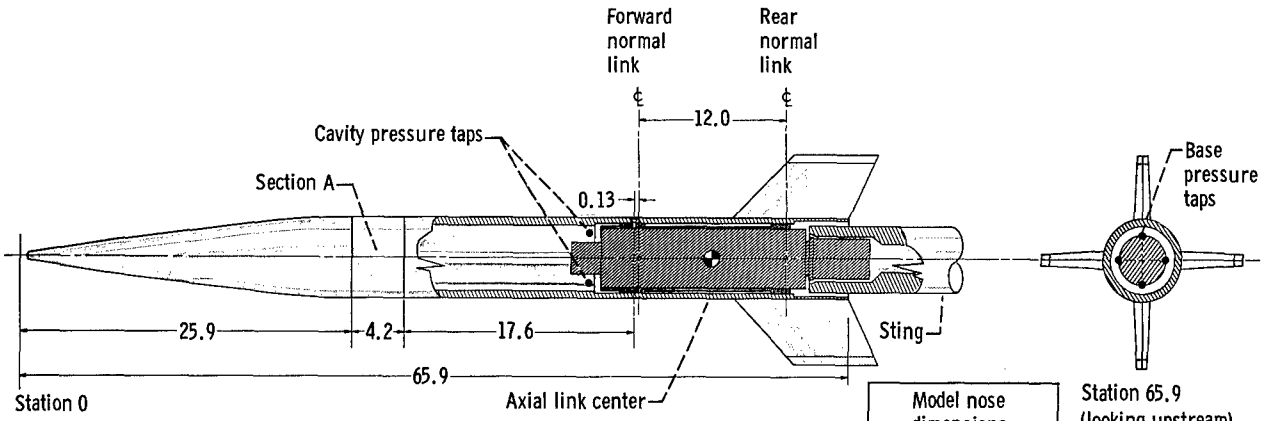

Model nose dimensions	
Station, in.	Radius, in.
1.143	.306
1.905	.449
3.810	.754
5.714	1.023
7.619	1.278
9.524	1.523
11.428	1.759
13.333	1.986
15.238	2.204
17.143	2.414
19.048	2.614
20.952	2.793
22.857	2.927
23.810	2.970
24.000	2.975
24.762	2.994
25.900	3.000

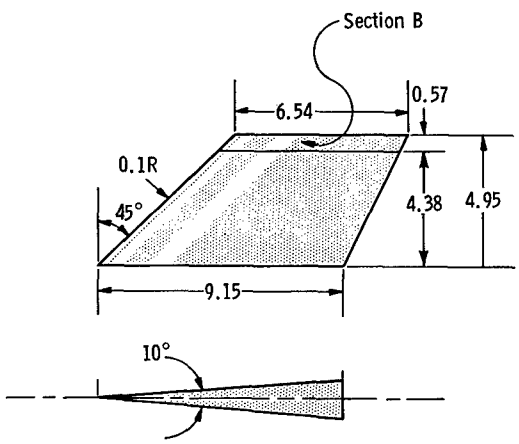

Figure 1. - Sketch of model A. Section A removed from model A for model B, 61.7 inches long; section B removed from model B for model C, with 70.34-square-inch planform area. (All dimensions in inches.)

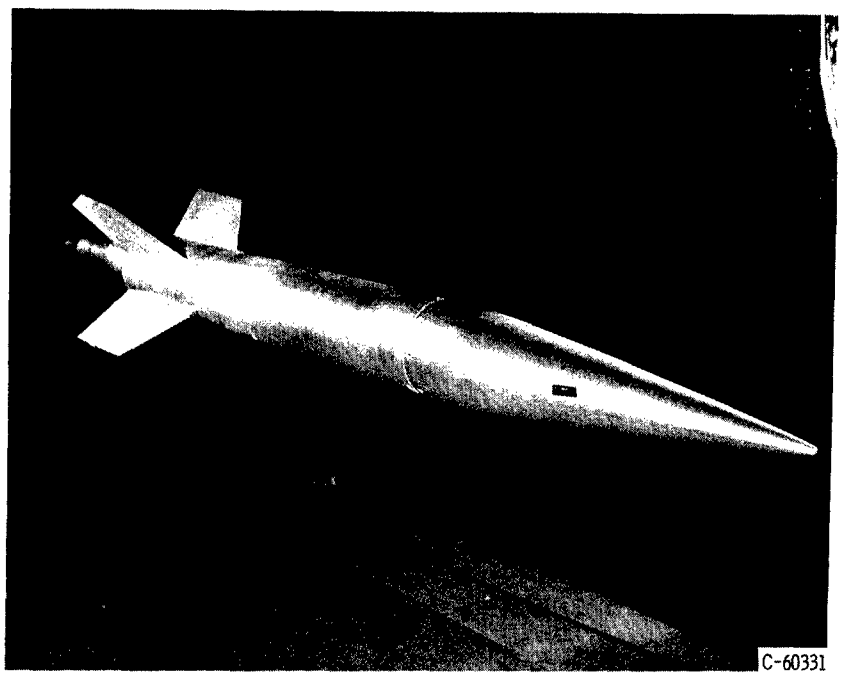

Figure 2. - Model B mounted in 10- by 10-foot supersonic wind tunnel.

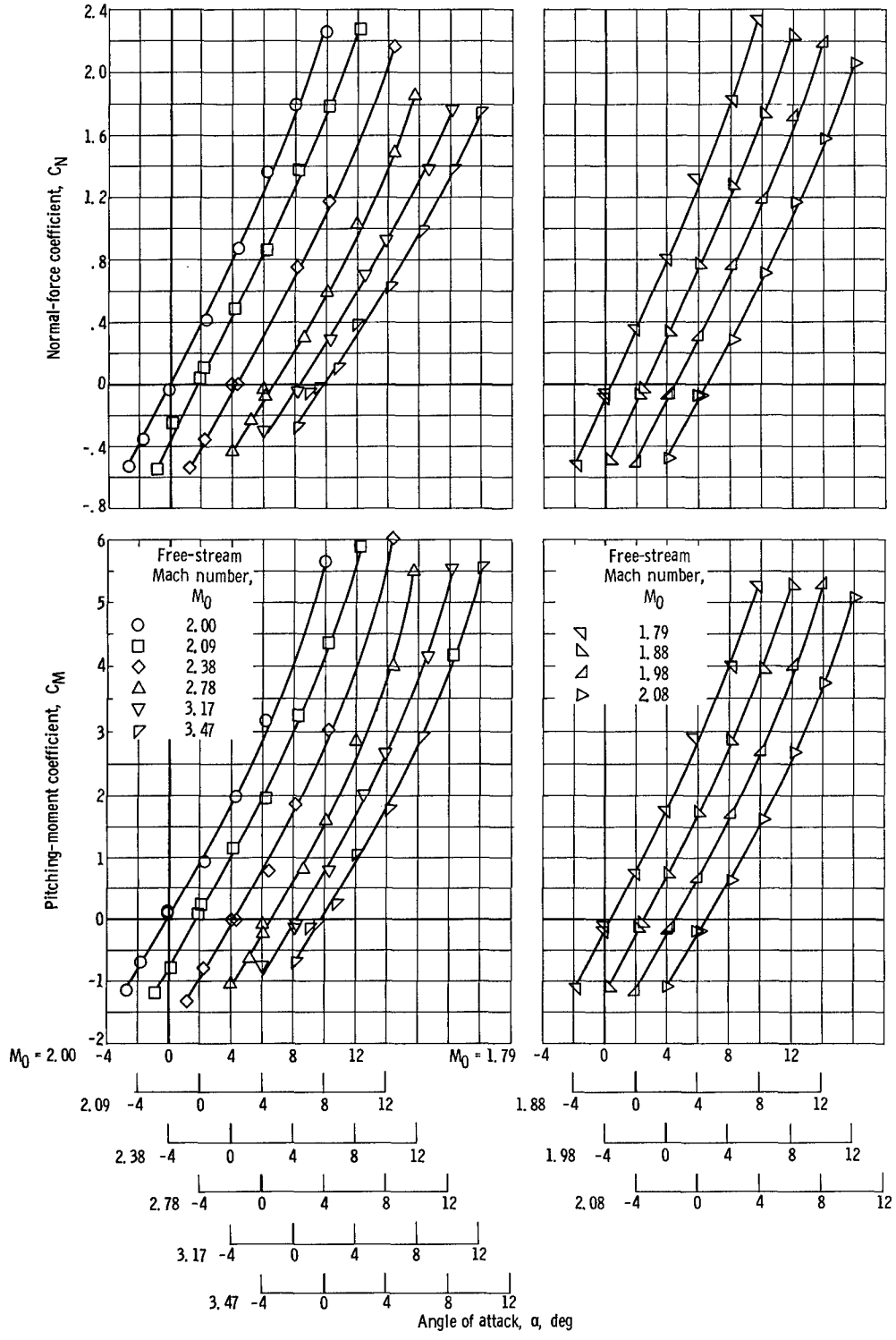

(a) Model A, 0° roll; 10-by 10-foot supersonic wind tunnel.

(b) Model A, 0° roll, 8- by 6-foot supersonic wind tunnel.

Figure 3. - Force and moment coefficients.

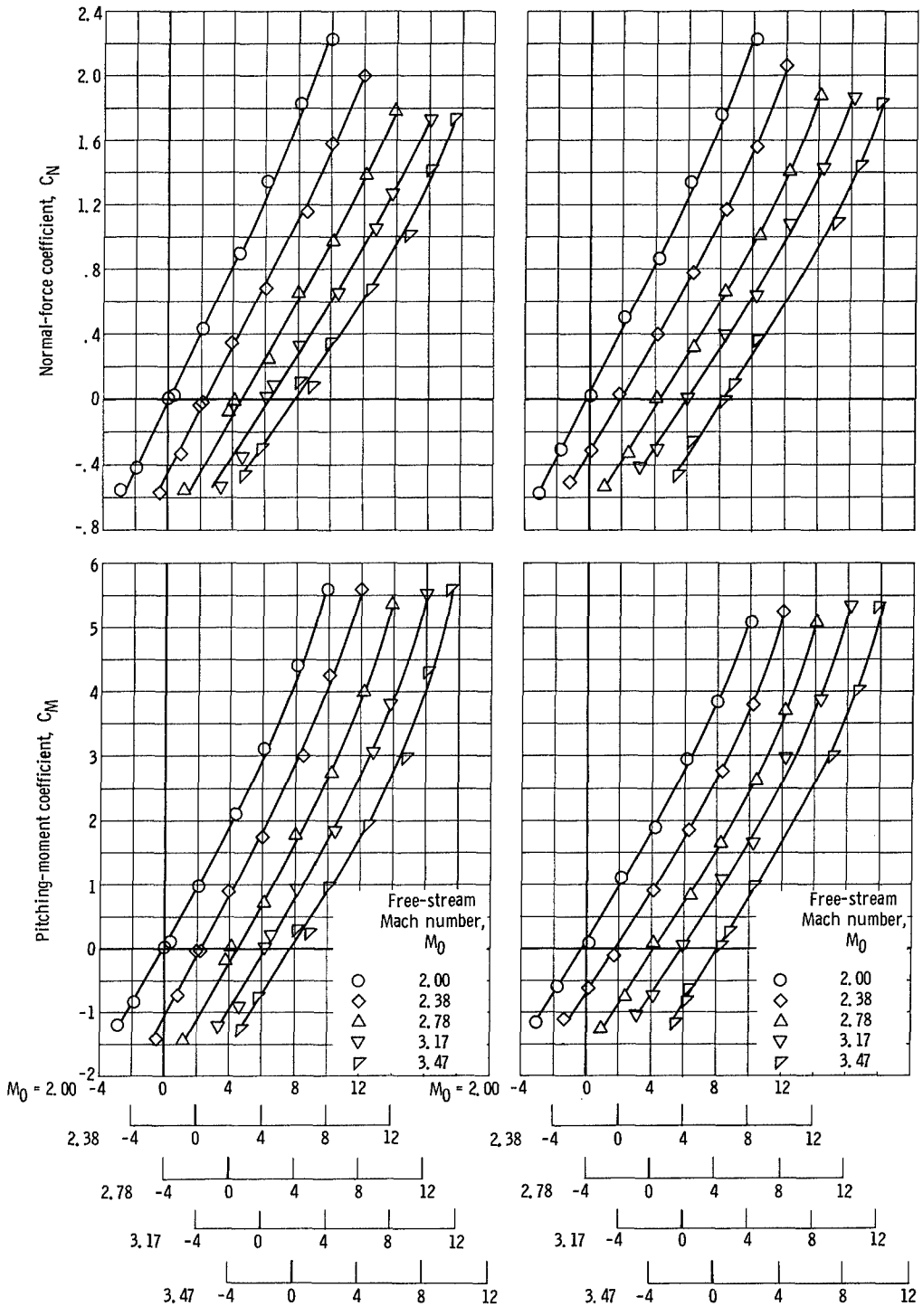

(c) Model A; 45° roll; 10- by 10-foot supersonic wind tunnel.

(d) Model B; 0° roll; 10- by 10-foot supersonic wind tunnel.

Figure 3. - Continued.

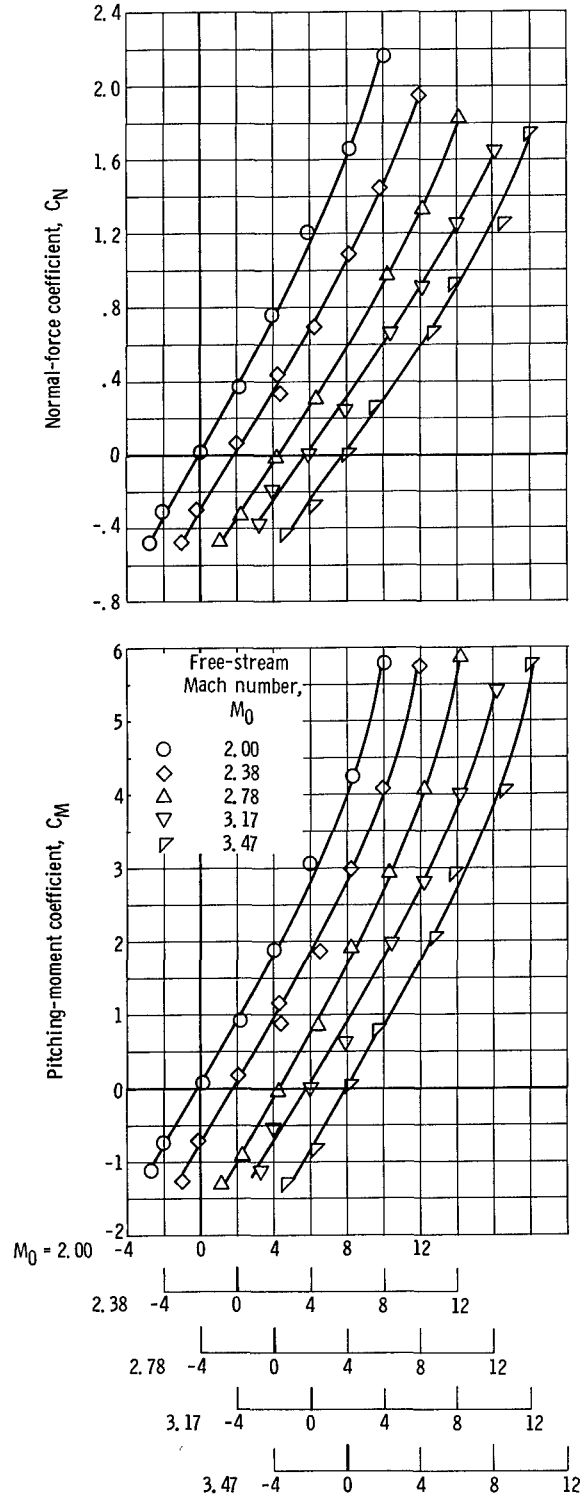

(e) Model C; 0° roll; 10- by 10-foot supersonic wind tunnel.

Figure 3. - Concluded.

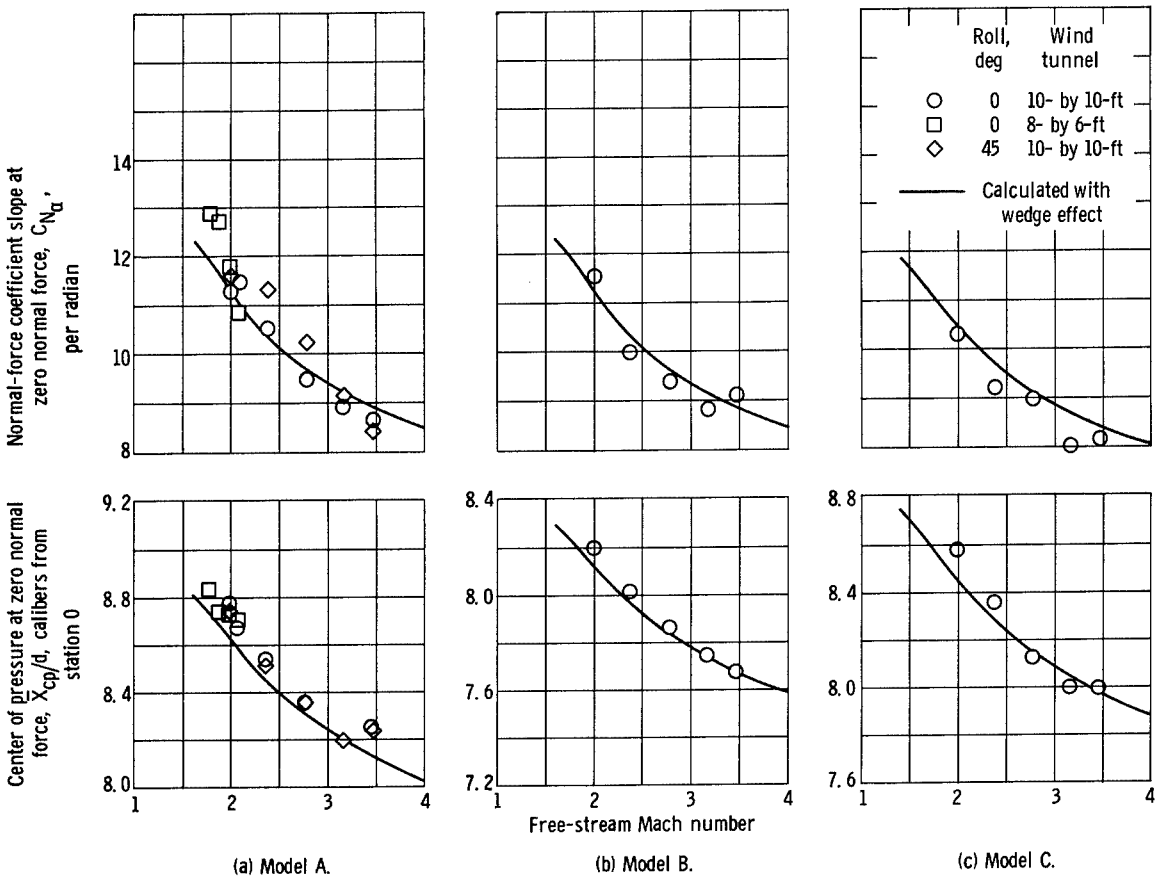

Figure 4. - Comparison of test results and calculated values of longitudinal static stability characteristics.

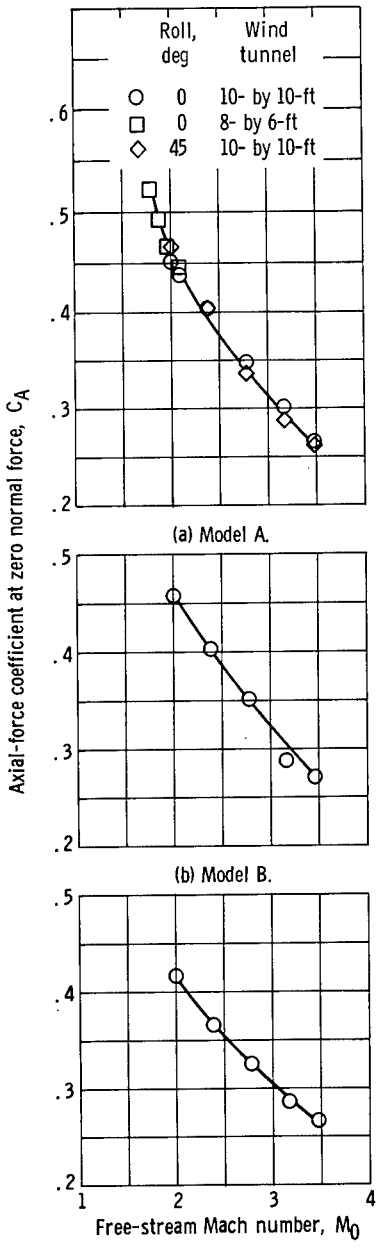

Figure 5. - Axial force coefficient as function of Mach number.

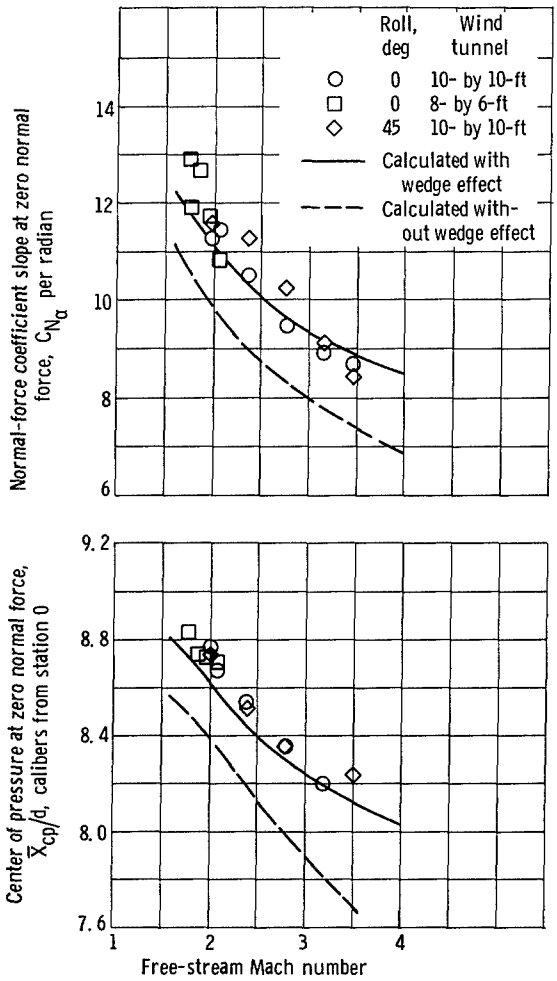

Figure 6. - Comparison of calculated values with wedge effect and without wedge effect for longitudinal static stability characteristics for model A.

NASA-Langley, 1966 E-2774